Development and applications of compact high-intensity lasers*

G. Mourou† and D. Umstadter
Center for Ultrafast Optical Sciences, University of Michigan, Ann Arbor, Michigan 48109-2099

(Received 18 December 1991; accepted 12 March 1992)

The development of compact high-intensity lasers, made possible by the technique of chirped pulse amplification, is reviewed. This includes the complexities of high-power laser implementation, such as the generation of short pulses, pulse cleaning, wide-bandwidth amplification, temporal stretching and compression, and the requirements for high-average powers. Details of specific solid-state laser systems are given. Some applications of these lasers to short-pulse coherent short-wavelength [x-ray ultraviolet (XUV)] sources are also reviewed. This includes several nonlinear effects observed by focusing a subpicosecond laser into a gas; namely, an anomalous scaling of harmonic generation in atomic media, an upper limit on the conversion efficiency of relativistic harmonics in a plasma, and the observation of short-pulse self-focusing and multifoci formation. Finally, the effects of large ponderomotive pressures (100 Mbars) in short-pulse high-intensity laser–plasma interactions are discussed, with relevance both to recombination x-ray lasers and a novel method of igniting thermonuclear fusion.

I. INTRODUCTION

It is now possible with the technique of chirped pulse amplification to build compact solid-state lasers that produce ultrashort pulses with intensities three to four orders of magnitude higher than was previously possible. These pulses have multiterawatt peak power, and when focused can produce intensities in the range of 10^{18} W/cm^2. The electric field at the laser focus at this intensity is approximately 3×10^{10} V/cm. Since this greatly exceeds the Coulomb electric field seen by the valence electrons, it results in both collisionless ionization without tunneling, and highly nonlinear interactions with bound electrons. For 1 μm light, the field is high enough, in fact, to cause plasma electrons to oscillate at relativistic velocities, and thus exhibit highly nonlinear motion due to the magnetic component of the Lorentz force. For the first time, this allows the study of nonlinear optics involving free electrons. These pulses also have extremely short time durations, in the range of 100 fsec to 1 psec. Since this is shorter than the timescales of either significant hydrodynamic motion or thermal equilibration, short-scale length, solid-density, and nonequilibrium plasmas may be produced. Furthermore, the high-average powers of these lasers make possible the use of sampling techniques to study inherently statistical phenomena. Applications of these novel laser interactions include the generation of coherent x-ray ultraviolet (XUV) radiation, the ignition of laser-fusion targets, and the acceleration of electrons. In this paper, we will present the state-of-the-art for ultraintense laser pulse generation using chirped pulse amplification, and discuss some of their current and potential applications in the field of—what has become known as—high-field science. Most of the work that will be discussed is ongoing at the National Science Foundation Center for Ultrafast Optical Sciences (CUOS).

The paper is divided into two major sections: one describing issues in the development of high-intensity lasers (Sec. II) and the other, their applications to high-field science (Sec. III). We begin with a general discussion of chirped pulse amplification in Sec. II A, followed in Sec. II B by a specific discussion of the important issues involved its implementation: the generation of clean pulses, stretching and compression, and large-bandwidth amplification. In Sec. II C, we will discuss current and future high-average-power systems. Section III begins with an overview of the applications of these lasers (Sec. III A), discussing in particular their relationship to laser intensity and pulse width. We then discuss some specific applications: harmonic generation in atomic and ionized media (Sec. III B), self-focusing and multifocus formation (Sec. III C), and finally, the dominance of light pressure in the dynamics of high-intensity laser–plasma interactions (Sec. III D).

II. HIGH-INTENSITY LASER DEVELOPMENT

It is a tribute to scientific and engineering ingenuity that—due to a series of breakthroughs—the laser has, since its inception, produced ever higher power pulses. In 1960, free-running lasers were capable of delivering kilowatt pulses. A few years later, Q-switching made the generation of power into the megawatt regime possible. Finally, in 1965, gigawatt pulses were demonstrated by using mode-locking techniques (see Fig. 1). Given this rapid rate of development, it was reasonable to expect that by the end of the 1960s, new theoretically predicted phenomena would be observable experimentally as terawatt pulses became available. Unfortunately, these early hopes did not materialize. For more than 20 years, the peak power of compact solid-state laser systems remained at the gigawatt level. This situation, however, changed in 1985, after the first demonstration of a new type of amplification technique, namely, chirped pulse amplification (CPA).[1] Now that la-

*Paper 4IG4, Bull. Am. Phys. Soc. **36**, 2374 (1991).
†Invited speaker.

 0899-8213/92/072315-11$04.00

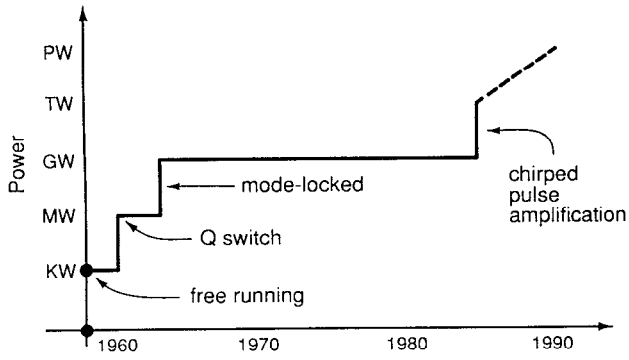

FIG. 1. Peak-power capability of small aperture [$O(\mathrm{cm}^2)$] laser amplifiers has increased stepwise through the years.

sers employing this technique have become readily available, a new era of discovery—similar to that following the invention of the laser itself—has begun. Other high-intensity laser systems not employing CPA will not be discussed, since they do not use solid-state materials, and thus do not qualify as compact.

A. Chirped pulse amplification

The amplification of short optical pulses to high-energy levels requires the fulfillment of three conditions. First, the bandwidth of the gain medium should be broad enough to accommodate the laser pulse spectrum. Second, the amplifying medium should have superior energy storage. Third, the laser intensity should be kept low enough to avoid nonlinear wave-front distortion.

The first condition originates from both the relationship between the laser pulse width and its bandwidth, given by the Fourier transform, and gain narrowing due to the finite bandwidth of the amplifier. The former is given by the relation $\Delta\nu\tau\sim 0.5$, where $\Delta\nu$ is the bandwidth and τ is the pulse duration. If it were not for gain narrowing, this would correspond to a lower limit on the wavelength bandwidth of 16 Å for a 1 μm picosecond pulse. However, because of the frequency dependence of the gain medium, the various frequencies that comprise the laser pulse are unequally amplified, leading to a reduction of the pulse bandwidth (gain narrowing), and, consequently, to an increase of the output pulse duration. For a 1 μm picosecond pulse, gain narrowing imposes a lower limit on the gain bandwidth of several hundred angstroms.

The second has to do with energy storage and efficient energy extraction. The latter requires an input fluence of the order of the saturation fluence F_s to efficiently extract the energy stored in the amplifying medium $F_s = h\nu/\sigma$, where h is Planck's constant, ν is the frequency of light, and σ is the stimulated emission cross section. For example, the saturation fluence of dyes and excimers, due to the large emission cross section, is of the order of $\mathrm{mJ/cm}^2$. On the other hand, it is much larger, i.e., of the order of 1 $\mathrm{J/cm}^2$, for media such as Nd:glass, Ti:sapphire (Ti:Al_2O_3), and alexandrite, which have low emission cross sections. For a pulse of duration $\tau=1$ psec, this fluence corresponds to intensity level $I=F/\tau$ of 1 $\mathrm{GW/cm}^2$ for dyes and excimers and 1 $\mathrm{TW/cm}^2$ for Nd:glass, Ti:sapphire, and alexandrite.

The third amplification condition, that the laser intensity should be kept low enough to avoid nonlinear wave-front distortion, imposes an upper limit on the laser pulse intensity. This limit stems from the intensity-dependent index of refraction leading to nonlinear wave-front distortion of the beam. The spatial inhomogeneities on the beam will grow at an exponential rate g given by the gain coefficient[2]

$$g=(k/n_0)(\lambda/2\pi L)B, \tag{1}$$

for $k<300\ \mathrm{cm}^{-1}$, where k is the spatial wave number, λ the light wavelength, n_0 the medium index of refraction, and L the length of the optical medium. The number of waves of nonlinear phase shift accumulated in traversing the amplifying medium is usually expressed by the factor B given by

$$B=\frac{2\pi}{\lambda n_0}\int_0^L n_2 I(z)dz, \tag{2}$$

where n_2 is the nonlinear index of refraction. To maintain the beam quality, it is essential to keep B to a minimum. A common practice in laser-fusion class systems, is to spatially filter the beam whenever the value of B reaches 3–4,[3] corresponding to an accumulated wave-front distortion of approximately $\lambda/2$. However, for short-pulse applications, where the highest on-target intensities are required, the beam quality requirements are more stringent, and a new criterion needs to be used. An expression exists, attributed to Marechal,[4] that defines the peak of the intensity I_p at the diffraction focus when the aberrations are sufficiently small. For the aberrations produced by nonlinear effects, this expression becomes

$$I_p\sim 1-B^2. \tag{3}$$

For a $B=0.7$, the intensity at focus will be reduced by a factor of 2. In order to generate a high-spatial quality beam, it is imperative to keep the intensity below this limit. Using conventional techniques, this condition could only be met in poor energy storage media, e.g., dyes and excimers, where the input intensity can easily be kept below this level without sacrificing energy extraction. On the other hand, for materials with good energy storage characteristics such as Nd:glass, Ti:sapphire, alexandrite, and Li:SaF, input fluence on the order of a $\mathrm{J/cm}^2$ is necessary to achieve efficient extraction. For example, for pulses of the order of 1 psec or less, that means intensities of the order of $\mathrm{TW/cm}^2$, which is by far above the acceptable level to maintain adequate beam quality. *This stored energy, however, can be extracted by first stretching, then amplifying, and finally compressing the short pulse, in a technique known as chirped pulse amplification (see Fig. 2).* We notice that, by stretching the pulse, we keep the input fluence constant while reducing the intensity.

The first terawatt level pulses produced using this technique were demonstrated by Maine *et al.*[1] Since then, CPA has been used successfully on larger laser systems in the

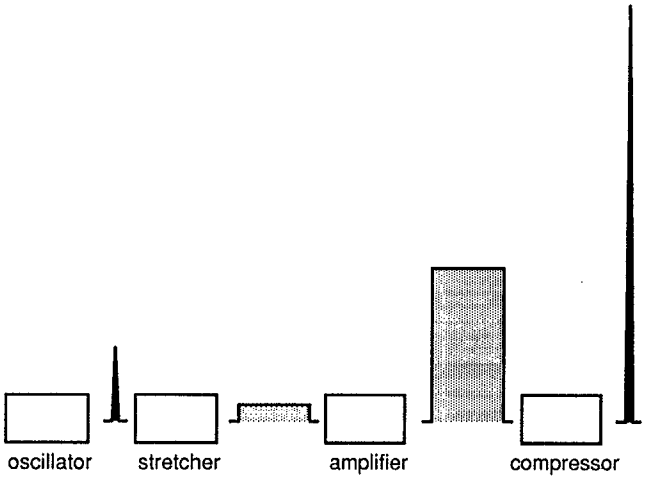

FIG. 2. In chirped pulse amplification, the pulse is temporally stretched in order to the lower peak intensity before amplification. After the stored energy is extracted from the amplifier, the pulse is temporally compressed to the initial duration. This allows the use of high-energy-storage materials for short-pulse amplification.

U.S.A. (10 TW),[5] France (20 TW),[6] and Japan (30 TW).[7] See other articles in this issue for details, including a discussion by Watteau *et al.* of the 20 TW laser system built at the CEA–Limeil in France in collaboration with the CUOS.

B. Tabletop terawatt (T^3) lasers

The CPA technique requires some impressive pulse manipulations: first, the generation of an extremely temporally clean short pulse; second, a stretching of this pulse by 1000 to 12 000 times; third, an amplification by a factor of 10^{10}, without pulse spectrum degradation; and finally, a pulse recompression by another factor of 1000 to 12 000 times. After all these elaborate manipulations, the laser pulse has to be close to diffraction limit, as short as the initial pulse, and still be temporally clean with a peak-to-background of at least 10^6:1. We will now discuss in detail each of these problems and their solutions.

1. The generation of ultraclean pulses

These solutions are presently embodied in a 1.6 TW Ti:sapphire/Nd:glass system that is currently in operation at CUOS.[8] A schematic of the front end of the laser system is shown in Fig. 3. The laser produces 640 mJ in 400 fsec pulses at 1.05 μm with an intensity contrast ratio of 5 $\times$ 10^5:1. The system consists of a 100 MHz mode-locked Nd:YLF oscillator producing 40 psec pulses. The output is sent into an 800 m, single-mode fiber. Through self-phase modulation and group velocity dispersion, the bandwidth and pulse width are increased to 42 Å and 110 psec, respectively. The pulse is then recompressed and sent to a pulse cleaner to improve the contrast ratio.[9] A high contrast is required to prevent the formation of a preplasma during the experiment. The pulse cleaner consists of a birefringent fiber between high-quality polarizers.[3] Owing to the nonlinear index of refraction in the fiber, the state of polarization of the light becomes intensity dependent. This can be used to discriminate between the low- and the high-intensity part of the pulse with a discrimination ratio of 10^6:1. Since the threshold for preplasma formation is $\sim$ 10^{12} W/cm^2,[10] this allows intensities up to 10^{18} W/cm^2 to be used in experiments. The transmission of the pulse cleaner for high intensity is of order unity. The pulse after

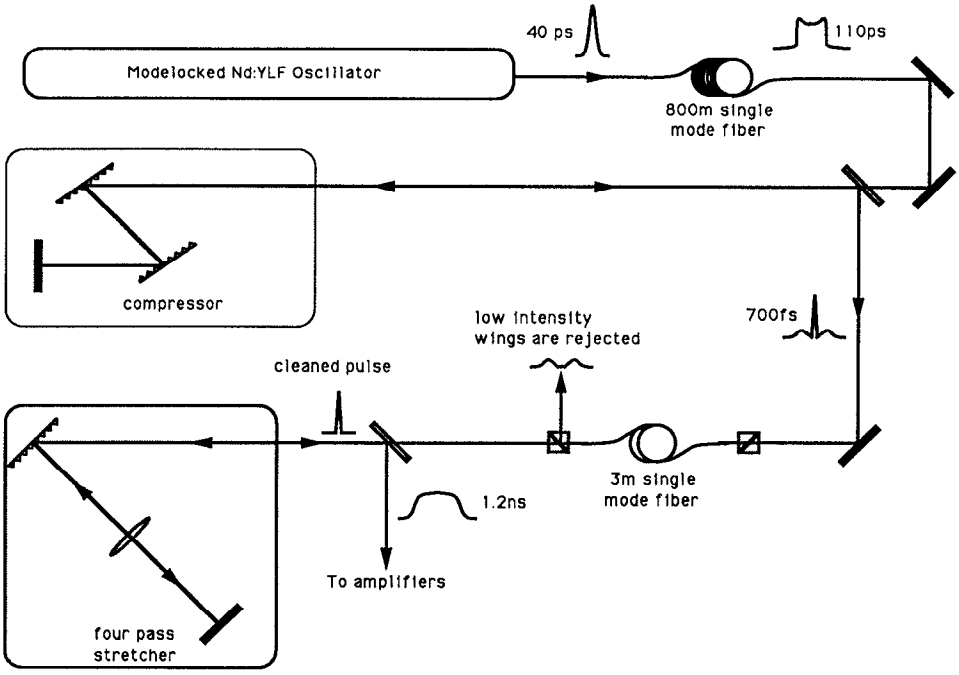

FIG. 3. Schematic of the front end of a CPA-based Nd:glass laser system configuration.

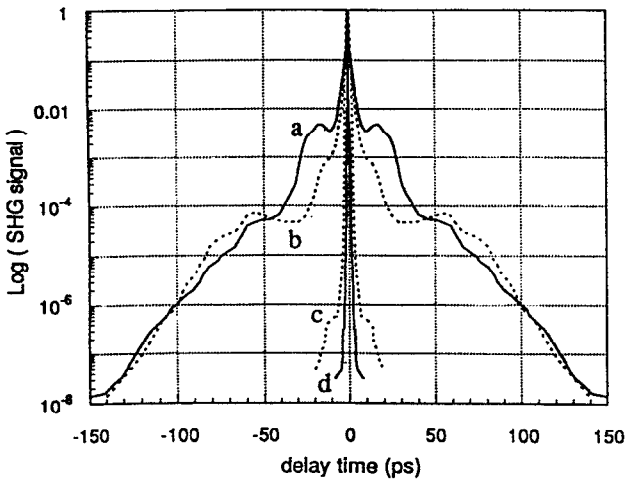

FIG. 4. A high dynamic range autocorrelation measurement: (a) after the first compression stage ($\tau_p = 700$ fsec); (b) same with a hard aperture for spectral windowing in the grating compressor; (c) direct output from the pulse cleaner; (d) after second compression stage ($\tau_p = 200$ fsec).

the grating-pair compressor has been measured over eight orders of magnitude with a high-dynamic range autocorrelator. Figure 4 shows the spectacular improvement that can be obtained by using this pulse cleaning technique. This technique departs from previously demonstrated ones, which use either Pockels cells[7] or saturable absorbers.[11] It is purely passive with a femtosecond-time response, unlike Pockels cells, and does not degrade the beam, unlike saturable absorbers.

This technique may be further enhanced by the replacement of the Nd:YLF oscillator with either a Kerr lens mode-locked Ti:sapphire oscillator,[12] or a Nd-doped-fiber oscillator.[13] Both of these have been shown to produce 100 fsec pulses at a wavelength of 1 μm, thus eliminating the need for fiber stretching. The pulses, once produced by the oscillator, can be further cleaned by the pulse cleaner. In this way, contrast ratios of greater than 10^{10} should be obtainable.

2. Pulse stretching and compression

Before amplification, the pulse must be stretched. For a large stretcher/compressor ratio R, the group-velocity dispersion of the fiber cannot be used for stretching because it cannot be exactly compensated (over all orders) by that of the grating pair compression stage. The mismatching between the two group velocity dispersions can lead to some unacceptable background [see Fig. 4(a)]. In 1987, Martinez proposed a grating pair compressor composed of gratings in an antiparallel configuration to compress pulses between 1.3 and 1.6 μm, stretched by negative group velocity dispersion in the fiber.[14] We demonstrated[15] that this grating configuration could also be used as a matched stretcher for our applications, with wavelengths shorter than 1.3 μm. We also demonstrated[16] that this grating-based stretcher/compressor system was matched to second order even for $R > 10^4$, a remarkable improvement over the initial fiber stretcher/grating compressor, which was limited to an $R < 100$. It is now one of the basic components of the CPA technique.

3. Large-bandwidth amplification

The stretched pulse is amplified before compression from the subnanojoule to the joule level, which is a factor of more that ten orders of magnitude. Our initial T^3 system was composed entirely of Nd:glass amplifiers, which have relatively narrow gain bandwidth [$(\Delta\lambda)_g = 250$ Å], limiting the final pulse duration to approximately 1 psec. Most of the gain narrowing occurs at the front end of our amplifier system, where the pulse is amplified by a regenerative amplifier from the subnanojoule to the millijoule level (gain of 10^7). This problem was recognized early, and we proposed[17] to use a combination of Nd:glass to broaden the gain bandwidth, a suggestion that was eventually used by others.[18] We later replaced the Nd:glass by Ti:sapphire in the regenerative amplifier.[19] Ti:sapphire has an extraordinary large gain bandwidth [$(\Delta\lambda)_g \sim 2000$ Å] centered at 8000 Å and extending up to 1 μm. By this replacement, the gain-bandwidth problem encountered with Nd:glass is completely eliminated, and the final pulse width is limited only by the subsequent amplification stages, which only amplify the pulse by a factor of 10^3, from the millijoule to the joule level. After the last amplifier (16 mm diam) the pulse has a duration of 1 nsec and an energy level of 1 J. Finally, the pulse is compressed by a double-pass grating system that is matched with the grating pulse stretcher.[8] In order to achieve the transform-limited pulse duration, the angles of incidence of the beam on the gratings have to be identical to within a tolerance of much less than a degree, with the required accuracy increasing with decreasing pulse width.

After compression, the pulse is 400 fsec in duration and has 600 mJ of energy, the latter being limited only by the size of the final amplifier and compression gratings. This exceeds a power of 1 TW. The pulse contrast is measured by a third-order autocorrelator[20] to be better than 10^5:1 (see Fig. 4). The beam spatial quality has been measured to be better than twice diffraction limited. At this power level, beam spatial quality is limited not so much by the laser but by the nonlinear propagation in air to the experimental chamber. We are currently working on installing vacuum beam lines to mitigate this problem.

C. Higher-average powers

1. Kilohertz repetition rates

One of the main advantages of the CPA technique is that it has made high peak power lasers available, because of their compact size, to a wider research community than before, when their availability was confined to large national labs. Thus their applications, including compact coherent x-ray sources, will extend to hospitals, universities, and research laboratories worldwide. For many applications in which sampling and averaging techniques are used, high-average powers are required. Toward this end, paral-

lel to the glass laser development discussed in Sec. II B, we have built CPA systems that use exclusively Ti:sapphire oscillators and amplifiers. While they cannot match the glass lasers in energy per pulse, these systems take advantage of the large bandwidth of Ti:sapphire to both generate and amplify 100 fsec pulses up to the 100 mJ level, and do so at 10 Hz.[21,22] Although this permits TW power levels at 300 times the repetition rate of the glass system, the energy per pulse of this system is inherently limited by the short upper-level lifetime of 3 μsec. At even higher repetition rates, a multikilohertz Ti:sapphire ($Ti:Al_2O_3$) amplifier for high-power femtosecond pulses has been demonstrated at CUOS.[23] The $Ti:Al_2O_3$ regenerative amplifier is pumped with a frequency-doubled Nd:YLF oscillator. At a 1 kHz repetition rate, the laser produces 1 mJ per pulse, and at a 7 kHz rate, it produces 85 μJ per pulse. This corresponds to a 1 W average power, which is two orders of magnitude above dye amplifier systems operating at equivalent repetition rates. The pulse width is 150 fsec, independent of the repetition rate. At the present time, work is being done to extend both the repetition rate and energy per pulse of this system.

2. Toward 10 TW tabletop (T^4) systems at a hertz

For applications requiring both high-average powers and energetic pulses, two laser-pumped systems, alexandrite-pumped Nd:glass and alexandrite-pumped Cr:LiSAF, are under development.[24] Flashlamp-pumped glass systems provided the necessary energies, on the order of a joule, but are limited in repetition rate because of thermal effects. Laser pumping can deposit the pump energy more efficiently. For instance, the average power of the current flashlamp-pumped T^3 system is on the order of 30 mW. On the other hand, we are developing an alexandrite-pumped T^3 Nd:glass system, which will potentially have an average power of 1–10 W. Several factors make these combinations of solid-state materials well matched. First, the Nd:glass has a long upper-level lifetime, ranging from 300–500 μsec, which is well matched to the pulse width of free-running alexandrite, 100 μsec. Second, good optical quality Nd:glass covering the spectrum from 1.04–1.09 μm can be obtained, making possible the amplification of pulses as short as 30 fsec with the proper choice of glasses. Third, the absorption band of Nd:glass is around 750–800 nm, well matched to alexandrite's tunable range. Finally, alexandrite can deliver an average power of up to 100 W (Ref. 24) with tens-of-joules energy per pulse.[25] We hope in the near future to have terawatt pulses at a few hertz, corresponding to 1 W average power.

Similarly, we are developing an alexandrite-pumped Cr:LiSAF system,[26] which takes advantage of the superior upper-level lifetime (70 μsec) and thermal properties of Cr:LiSAF. It should be capable of even greater repetition rates and still maintain joule-level energies. To date, millijoule CPA systems at 2–5 Hz have been demonstrated in both materials,[26] by our group and researchers at Allied Signal Corp.

III. APPLICATIONS TO HIGH-FIELD SCIENCE

A. Overview

The invention of the laser has, of course, had enormous impact on the fields of chemistry, biology, and physics. More recently, ultra-short-pulse lasers have spawned the field of ultrafast science. Now, with the development of high-intensity lasers the same has happened for another field, high-field science.[27] By combining high intensity with short pulses, their interactions with matter are unique. On the horizon, is the possibility of extending these tabletop short-pulse coherent sources to the short-wavelength region of the spectrum,[28,29] where no such compact sources currently exist. Once available, they too are expected to rapidly generate new research areas.

Recent progress toward this goal is promising. For instance, high-order odd harmonics, with frequencies extending well into the XUV region of the spectrum, have recently been generated by focusing intense lasers of the type discussed in Sec. II B into a gas.[30] While the observations are not currently well understood, what is most exciting is that rather than falling with harmonic number at the rate that would be expected from perturbation theory, a plateau has been observed in the conversion to higher harmonics.[30] Most of the work thus far in this area has been at intensities below the ionization saturation threshold,[31] and thus falls into the realm of nonlinear optics with bound electrons. However, work at CUOS has recently begun at greater intensities.[32] As will be discussed in detail below, in this case, a rich variety of nonlinear phenomena involving free electrons may be studied. Another path to coherent XUV generation is through the inversion of an ionic medium. The multifocus formation in gases, which will be presented in Sec. III C, has obvious applications here. The effects of the ponderomotive pressure (Sec. III D) has relevance as well. Before discussing each of these issues in detail, however, we will first attempt to provide some perspective by qualitatively discussing their dependence on various laser parameters, specifically, intensity and pulse width.

1. Intensity dependence

Different physical processes are distinguished by their dependence on the laser field.

(1) For instance, rapid disintegration of a hydrogen atom occurs as the laser field becomes comparable to the Coulomb field, $E_0 \sim e/a_0^2$ [$(3 \times 10^9$ V/cm or $I = 10^{16}$ W/cm^2)], where a_0 is the Bohr radius. Highly nonlinear multiphoton processes such as atomic harmonic generation[31] and tunneling ionization become important at weaker fields as the orbit of the electron becomes significantly perturbed by the presence of the laser.

(2) Light pressure should play an important role in plasma dynamics[33] when the gradient of the ponderomotive pressure $n_e m\langle v_{os}^2\rangle$ becomes comparable to the gradient of the plasma thermal pressure $(3/2)n_e kT_e$. In the laser interactions with solid targets presented in Sec. III D, the gradients are roughly comparable, and only the ratio of the quiver velocity ($v_0 = eE/m\omega$) to the thermal velocity [v_e

$= (kT_e/2m)^{1/2}$] matters. For the laser–plasma parameters discussed in those interactions ($T_e \sim 200$ eV, and $\lambda = 1$ μm), this ratio is approximately unity if E_0 again equals a value close to the Coulomb field. At somewhat higher fields, the enormous ponderomotive pressures of a short-pulse laser may provide a novel means for igniting thermonuclear reactions[34] (see Sec. III D).

(3) The mass of an electron should become modulated by relativistic effects, and thus its motion becomes highly nonlinear when v_0 approaches c, the speed of light. The required value of E_0 for $\lambda = 1$ μm is found to be equal to the highest attainable with current laser technology [(3×10^{10} V/cm or $I = 10^{18}$ W/cm^2)]. This results in the generation of relativistic harmonic radiation[35] and large amplitude wake-field plasma waves[36,37] with extremely high longitudinal electric fields that may be used to accelerate electrons.

(4) Finally, quantum electrodynamic effects, such as pair production, will become important when the work done by the laser electric field over a distance of a Compton wavelength, $\lambda_C \hbar/mc$, equals the rest mass of an electron, m_0c^2. This requires that E_0 equal a value that will be difficult to achieve even in the forseeable future [(3×10^{16} V/cm or $I = 10^{30}$ W/cm^2)].

Although the field strength required for the catastrophic production of electron–positron pairs from the vacuum is six orders of magnitude higher than is currently available with even the most intense lasers, the observation of a statistically significant number of pairs is predicted to occur at fields as low as $E_0 \sim 10^{14}$ V/cm.[38] The fact that the electric field in a frame moving with a relativistic electron beam is increased by γ, where γ is the relativistic factor associated with electron beam, may allow the observation of pair production with current laser technology.[38] For a 20 GeV electron beam, the field is increased by a factor of 4×10^4, and so, in this case, the threshold for observation of pair production can be exceeded with current technology. Another interesting effect permitted by the interaction of a high-intensity laser with a relativistic electron beam is nonlinear Compton scattering, which may generate photons with energies near the energy of the electron beam. In the case of a 20 GeV beam, this is in the gamma-ray region of the spectrum.[39]

2. Pulse width dependence

Similarly, as the laser pulse width is reduced, different physical regimes may be distinguished by comparing the pulse width (τ_L) to various characteristic timescales. With short pulses focused onto a solid target, it may be possible to deposit the bulk of the laser energy near the solid-density region.[40,41] This must be done in a time shorter than the time it takes the density scale length [$l_n \equiv n(dn/dx)^{-1}$] to evolve significantly due to hydrodynamic motion at close to the ion sound speed c_s. To our knowledge, an explicit criterion for this to occur has never been clearly stated. We suggest that this upper limit on the pulse width should be roughly the time it takes for the density scale length to become comparable to an optical skin depth (c/ω_p). This may be written as $\tau_L \leqslant (c/c_s)/\omega_p$, which, for typical laser–plasma parameters mentioned below, corresponds to a few hundred femtoseconds. Short-pulse interactions with 1 μm light are also unique because the density scale length remains less than a laser wavelength during the pulse duration. Important consequences of this are, for experimentalists, that it isolates plasma instabilities, and, for theorists, that the Wentzel–Kramers–Brillouin (WKB) approximation breaks down and exact solutions of the wave equation are required.[42]

Another important time scale is that for the ionization stages and electrons to thermally equilibrate, which at solid density can be on the order of 100 fsec. When the laser energy is deposited in a time shorter or comparable to this timescale, highly nonequilibrium plasmas may be generated, which may, in turn, result in population inversions through recombination and, ultimately, x-ray lasing action.[42,43] Finally, the timescale of the upper-state lifetime of an XUV transition is less than a few picoseconds, and so short-pulse high-intensity lasers should make efficient pumps for short-wavelength lasers.[45]

B. Harmonic generation

Nonlinear motion of electrons oscillating in the field of a laser will generate frequencies at odd harmonics of the laser frequency. If a laser is focused to a relatively low intensity onto a gas,[31] nonlinear motion of the electrons that are bound to the nucleus will be caused by the anharmonic atomic potential. At intensities exceeding the threshold for ionization, a plasma will be formed. A theoretical suggestion has been made recently that the ionization process, by generating nonlinear currents at twice the laser frequecy, may also produce odd harmonics.[46] At the highest laser intensities, nonlinear motion of unbound electrons occurs because of their relativistic mass change as their quiver velocity approaches the speed of light. This leads to the generation of harmonic radiation either incoherently, by laser-induced spontaneous radiation from individual electrons (Thomson scattering),[47] or coherently, by laser-driven plasma currents,[35] as discussed in another paper in this issue by Sprangle and Esarey.

The goal of the experiment discussed in Sec. III B 1 (Ref. 32) was to conduct a study of these processes by focusing a laser pulse into a gas to intensities far above the ionization saturation threshold I_S. In this case, the laser will interact with the gas at the front of the pulse and the edges of the focus, and will form a plasma in the central region. As will be discussed in detail, the scaling of the third harmonic with laser intensity that was observed in the experiment cannot be explained with conventional theories of bound-harmonic generation, and exhibits the same scaling that is predicted for relativistic harmonics.[32] Additionally, in order to explain the results of similar experiments, it has been speculated by others that a plasma may have been contributing to the harmonic production at intensities just above I_S (Refs. 48 and 49). In order to isolate these effects, we performed a pump-probe experiment, discussed in Sec. III B 2, in which an intense pulse interacted primarily with a preformed plasma. In so doing, we were able to eliminate relativistic plasma harmonic generation as

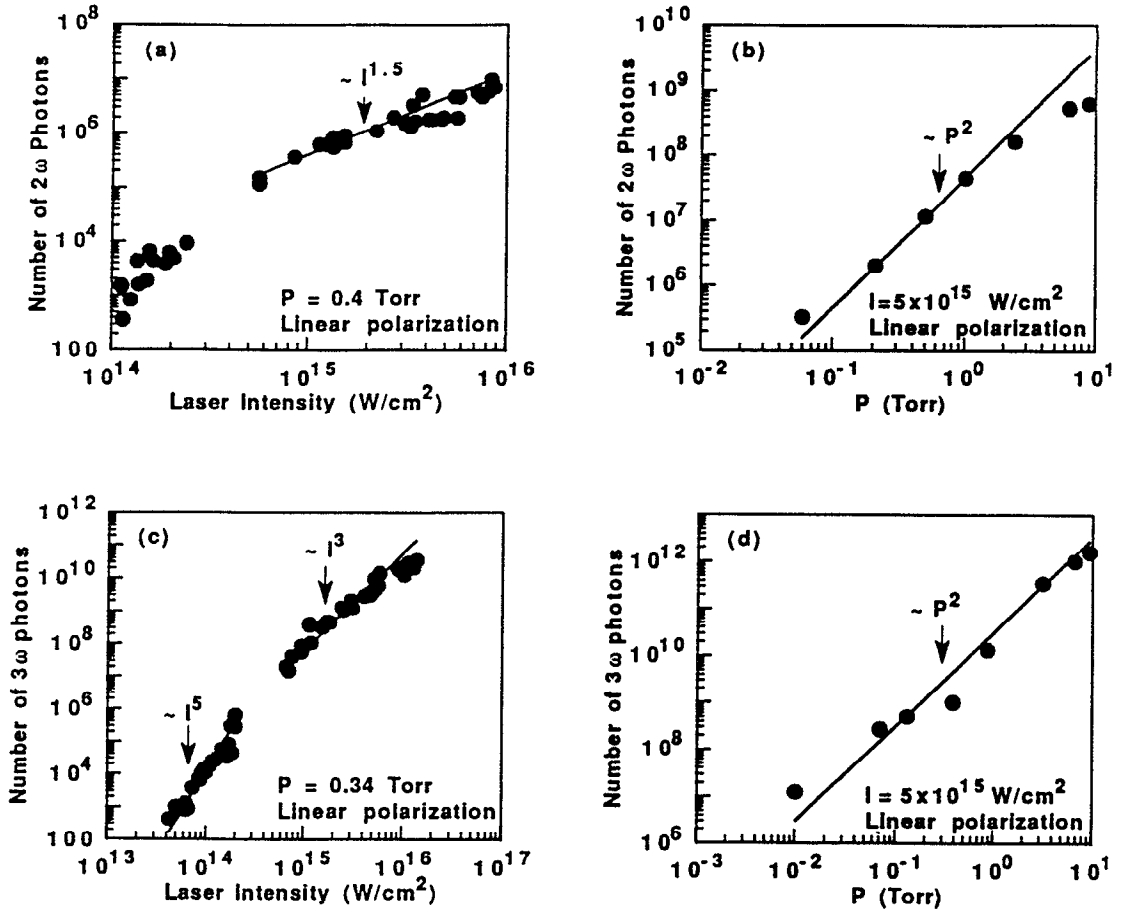

FIG. 5. Scaling of SHG and THG in a partially ionized hydrogen gas. (a) Below $I_S \sim 5 \times 10^{14}$ W/cm^2, SHG scales with intensity as $P_2 \propto I_0^{10}$. Above I_S, SHG scales as $P_2 \propto I_0^{3/2}$, indicative of volume ionization effects. The gap in the data was solely due to the detection method. (b) The measured scaling of SHG with pressure, $P_2 \sim p^2$, agrees with the predicted scaling of either Bethune's or the above theory. (c) Below I_S, the scaling of THG with intensity agrees with the theory of harmonic generation from bound electrons in a gas, $P_3 \propto I_0^5$. Above I_S, the THG scales anomalously as $P_3 \propto I_0^3$. (d) The measured scaling of THG with pressure is $P_3 \sim p^2$.

the cause of the observed anomalous scaling above I_S, and, simultaneously, establish an upper bound for the harmonic conversion efficiency by this mechanism.

1. Atomic harmonic generation

In the first experiment, a single pulse from a 1.053 μm CPA-based Nd:glass laser of the type discussed in Sec. II B was focused into a gas cell backfilled with hydrogen.[32] The scalings of second-harmonic generation (SHG) and third-harmonic generation (THG) with gas pressure for fixed intensity, or with intensity for fixed pressure—shown in Fig. 5—were measured with a photomultiplier tube and appropriate bandpass filters. The intensity at the focus was varied from a value that was much below to one that was much above the threshold for tunneling ionization. In the former case, the light pulse interacted with an atomic gas. In the latter case, the foot of the pulse rapidly ionized the gas and the rest—except for the wings of the Gaussian profile, transverse to the propagation direction—interacted with a fully ionized plasma. The effect of any residual ionization will be to further enhance the generation of coherent harmonics, as discussed by Brunel.[46]

As shown in Fig. 5(a), for a gas pressure of 0.4 Torr, the scaling of SHG at low intensities agrees with the prediction of Bethune,[50] in which P_2 should scale with intensity approximately as the number of photons required to ionize hydrogen (~ 10), $P_2 \sim I_0^{10}$. In this case, the origin of SHG is attributed to atomic effects associated with electric-field-induced third-order mixing driven by charge separation.[50,51,48] At higher laser intensities, SHG scales as $P_2 \propto I_0^{3/2}$. A similar change in scaling to one with $I_0^{3/2}$, described as saturation, has been observed in ion production.[52] This scaling is consistent with the expectations of theory. The exponent 3/2 arises from the increase in volume of the halo region of the laser focus, in which the gas is partially ionized.[52] The transition in the scaling in Fig. 5(a) indicates that the ionization saturation threshold intensity is $I_S \simeq 5 \times 10^{14}$ W/cm^2.

THG also scales differently above I_S than below it, as shown in Fig. 5(c), for a gas pressure equal to 0.34 Torr: below, it scales as $P_3 \propto I_0^5$, and above, $P_3 \propto I_0^3$. Under our experimental conditions, with a confocal parameter less than the length of a positively dispersive medium, third-harmonic generation is normally forbidden because of

phase matching.[49] Its observation, and even the I^5 scaling below I_S, which has been observed elsewhere,[51,49] are understood. It has been explained by invoking an argument that a laser-dependent nonlinear change in the refractive index (the Kerr effect) modifies the propagation and phase matching of the third harmonic.[51,49] Above I_S, the scaling is not understood. The THG does not saturate at a level that would be expected by considering volume ionization effects alone. In this case, a lower scaling—the same as is observed in SHG, $I_0^{3/2}$—would be expected. In fact, the cubic scaling is precisely what is predicted by a theory for relativistic harmonic generation.[32,35] However, we can rule out this last possibility by the results of a pump-probe experiment, presented in the next section, in which a laser interacted only with a plasma. Instead, a combination of volume ionization effects and the Kerr effect, or nonlinear currents from ionization,[46] may be required for an explanation. We hope this anomalous scaling will provide a fruitful direction for future theory.

2. Harmonic generation in plasmas

In order to study plasma harmonic generation by free electrons, without the competing effect of atomic harmonic generation by bound electrons, a preformed plasma was produced. This was accomplished by means of a pump-probe configuration, in which two collinear laser pulses of almost equal intensity but opposite polarizations were delayed with respect to each other by use of a delay line and then brought to a common focus with the same focusing lens. That they overlapped in space transverse to the direction of propagation was determined to an accuracy of better than 2 μm, or 5% of their focal diameters, by imaging their foci with a CCD camera and a microscope with a magnification factor of 15. The two laser pulses, each of 1 psec duration, were focused to intensities of 5×10^{16} W/cm^2 and 1×10^{16} W/cm^2, respectively, onto a pulsed molecular beam of hydrogen. This value for the intensity of the second pulse corresponds to a normalized vector potential of $a=0.1$, where $a = eE_0/mc\omega$. With this configuration, the first pulse creates the plasma in advance of the arrival of the second pulse. Hydrogen was chosen for the gas because its single-ionization stage. Since, for linear polarization, the direction of polarization of the harmonics is along that of the laser, and since the two pulses are polarized orthogonally, the harmonics generated by the second pulse, which interacts only with a plasma, may be distinguished by use of a polarizer from those that were generated by the first pulse, which interacts with the gas.

It was found that, with less than a 10 psec delay between the two pulses, much less than the recombination time at this density ($n_e \sim 10^{17}$ cm^{-3}), the second pulse produced a factor of 10^6 less third harmonic than in the case when the first pulse was blocked, and hence no preformed plasma was produced. *In other words, for our laser parameters, the power conversion efficiency for harmonic generation in a plasma formed only of electrons and protons is at least six orders of magnitude less than that in a neutral gas.* This translates into an upper bound on the conversion efficiency to third-harmonic generation by the mechanism of relativistic harmonic generation of $\eta_3 \leqslant 10^{-12}$. This is consistent with a value predicted by theory of $\eta_3 \leqslant 10^{-14}$ (see Sprangle and Esarey in this issue).

Future work will be concentrated on improving the dynamic range of this measurement, which is limited by two factors: first, the finite discrimination of the polarizer against residual third-harmonic of the opposite polarization from the first pulse, and second, bound-harmonic generation by the second pulse from neutral atoms at the edge of the focal volume. Other geometries are currently being investigated.

C. Self-focusing and Multifoci formation in a gas

The topic of laser beam self-focusing has generated considerable recent interest because it may provide the long-sought-after solution to the problem of extending a high-intensity laser interaction region for laser–plasma electron acceleration,[36,37] x-ray lasers,[28,53] and harmonic generation.[30] Focusing with cylindrical lenses has been used in the past to produce long interaction regions, but cannot be used to produce a high intensity at the laser focus over any significant distance.[54]

Self-focusing or self-defocusing, in either atomic or ionized media, originates from a radial intensity-dependent refractive index gradient. Self-focusing occurs when a negative gradient acts as a positive lens, and vice versa for self-defocusing. The mechanism responsible for the index change depends on the laser pulse duration and intensity. For continuous wave (cw) and long pulses, thermal,[55] ponderomotive,[53] and molecular orientational nonlinear effects[56] are dominant. For pulses of picosecond and shorter duration, only the electronic nonlinear susceptibility and ionization are important.[56] Furthermore, at extremely high laser powers, relativistic self-focusing must be considered.[35,57]

When a short-pulse laser is focused into a gas, a plasma will be formed wherever the intensity exceeds the ionization threshold. In the gas regions, a negative radial index gradient will be created by the intensity dependence of the nonlinear susceptiblity, focusing the beam. In the plasma region, a positive radial index gradient will be created by the intensity dependence of the ionization, defocusing the beam. A focused beam will also defocus because of diffraction, even without of an index gradient. A combination of these three effects may result in multiple self-focusing. Recently, at CUOS we observed multiple foci using an intense subpicosecond laser pulse.

The experimental setup was similar to those described above. Again, the laser was focused into a chamber backfilled with hydrogen. In order to image the location of the foci, light emitted from the laser-produced plasma was recorded with a digital CCD camera looking perpendicular to the laser axis. Beam propagation was investigated under various conditions: the focusing lens, the laser intensity, and the gas density were all varied. In this experiment, the power was much below the threshold for relativistic self-focusing.[57]

As the gas density was increased, the plasma column moved backward from the reference point toward the in-

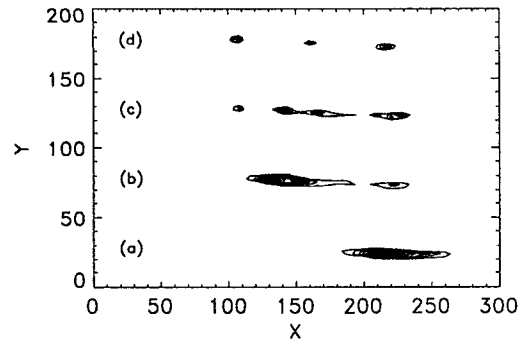

FIG. 6. Normalized plasma column images with $f=40$ cm lens in hydrogen: (a) $p=30$ Torr, 40 mJ; (b) $p=100$ Torr, 90 mJ; (c) $p=250$ Torr, 70 mJ; (d) $p=500$ Torr, 65 mJ. The beam propagates from left to right and the total distance along the propagation axis shown in the plot corresponds to 3 cm.

cident laser beam (see Fig. 6). As the gas density was increased further, a second focus developed, also backward toward the laser. As the gas density increased even further yet, three or more foci appeared [see Figs. 6(b)–6(d)]. The number of self-focused foci and their positions varied from shot to shot as the energy in the laser pulse fluctuated. The propagation was sensitive to the laser intensity and beam quality, but not the laser polarization. Some of the beam foci appear in Fig. 6 to be curved. We believe this is caused by nonlinear bending, also due to the nonuniformity of the incident laser beam.[58]

All of these observations were reproduced in numerical simulations in which the nonlinear Schrödinger equation was solved in the paraxial approximation. However, it was found that multifocus formation could only be simulated when we used values of the intensity-dependent nonlinear index that were much higher than those previously measured. Perhaps this extremely nonlinear behavior of the gas close to ionization, in which case higher-order terms may become important, is related to the anomalous scaling of the third harmonic above the ionization saturation threshold seen in Sec. III B 1.

D. Competition between ponderomotive and thermal pressures

Large absorption of laser light and rapid cooling of the plasma are both required for recombination x-ray laser schemes involving laser–solid interactions. These two processes depend strongly on the evolution of the electron-density profile during the laser pulse. The latter, in turn, is nonlinearly coupled to the high-intensity laser through the pressure that the light exerts upon the plasma near the reflection point. It has recently been shown at CUOS[33] that when the quiver energy of the electrons becomes comparable to the plasma thermal energy, light pressure dominates the plasma dynamics. This is the first such study in the regime in which the density scale length (d) is much less than the laser wavelength (λ), $d \ll \lambda$.

When a laser pulse interacts with an overdense plasma, the pump laser light is absorbed and reflected near z_c, the critical surface—the point of the profile where the electron density n_e equals the critical density n_c, where $n_c/n_e \equiv (\omega_0/\omega_p)^2 = 1$, ω_0 is the incident laser frequency, and ω_p is the plasma frequency. For densities greater than n_c, the light wave is evanescent and is attenuated exponentially in a skin depth. This has two consequences. One, local heating and ionization create a sharp electron thermal pressure gradient, driving expansion of the plasma into the vacuum; and two, the sharp laser intensity gradient creates a ponderomotive force oppositely directed to the expansion. Twice the momentum of the reflected laser light is imparted to the expanding plasma. Since z_c is moving relative to the laboratory frame, the reflected pump light is Doppler shifted by an amount proportional to the velocity of expansion of the plasma into the vacuum, $v_{\exp}$, equal to $\Delta\lambda/\lambda = -2(v_{\exp}/c)\cos\theta$, where θ is the angle of incidence of the laser. This Doppler shift may thus be used to determine the motion of the plasma.

The dynamics of the laser–plasma interaction may be described mathematically by the one-dimensional two-fluid conservation equations of mass density, momentum (with the ponderomotive force included), and energy.[41,59] These equations are coupled to a collisional radiative model for the ionization stages, a modified Spitzer–Härm model for heat conductivity, and the Helmholtz wave equation for the electric field.[33,59,60] The results of a computer simulation that used these equations will be discussed later. However, it may be shown from a simpler steady-state solution of the Helmholtz equation for an exponential density profile[33] that the ponderomotive force $n_e \nabla p_l$ equals the thermal force ∇P_e at z_c if the quiver energy of the electrons equals their thermal energy, or, equivalently,

$$m\langle v_{os}^2\rangle/2kT_e \equiv 3.2\times 10^{-13} I_{\rm inc}\lambda_0^2/kT_e \sim 1 \qquad (4)$$

($I_{\rm inc}$ is in W/cm^2, λ_0 is in μm, and kT_e is in eV). The electric field, and thus the quiver velocity, in the plasma were related to the incident light intensity $I_{\rm inc}$ in Eq. (4) both by the fact that as the light wave approaches z_c, the peak value of E^2 is swelled by a factor of about 3.6 over its vacuum value $E_{\rm inc}^2$, and by the relationship $I_{\rm inc} \equiv (c/8\pi)E_{\rm inc}^2$. Equation (5) tells us that the ponderomotive force will be important with our laser parameters and $kT_e \sim 200$ eV, since in this case the equality is satisfied.

The results of an experiment that we recently performed may be explained by the effects discussed above. In this case, frequency-doubled pulses ($\lambda=0.53$ μm) with maximum energy of 70 mJ and duration 1 psec were focused at normal incidence ($\theta=0°$) onto a solid target of aluminum. The back-reflected light was sampled with a beam splitter that was placed before the target in the path of the laser and spectrally analyzed with a spectrometer coupled to a multichannel analyzer. A Doppler shift to the blue and a broadening—characteristics of an expanding plasma—were observed and are shown in Fig. 7(b) for the same intensity used in the experiment, $I_{\rm inc} \sim 2\times 10^{15}$ W/cm^2.

The measured Doppler shift, shown in Fig. 7(b), agrees quite well with a Doppler shift predicted by the above-mentioned simulation, as shown in Fig. 7(c), given the measured incident light spectrum shown in Fig. 7(a).

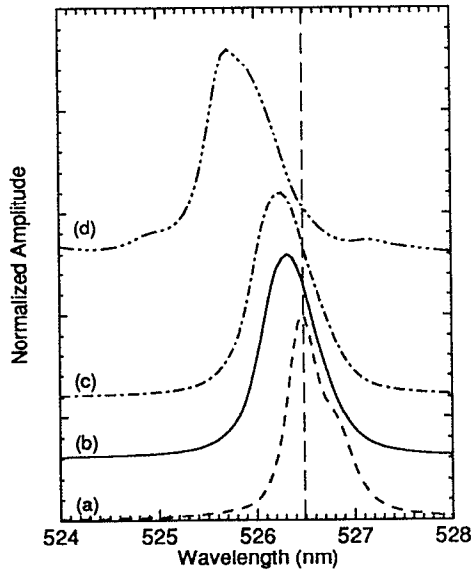

FIG. 7. The dynamics of the plasma is dominated by light pressure when the oscillatory energy of electrons in the field of the laser exceeds their thermal energy. (a) Spectrum of the light incident on the target. Doppler-shifted spectrum of the light reflected from the moving critical surface: (b) measured experimentally; (c) calculated numerically with the ponderomotive force included; (d) calculated numerically without the ponderomotive force.

That the free expansion model is inadequate is dramatically demonstrated in Fig. 7(d), which shows the Doppler shift calculated in the simulation without the ponderomotive force included. It is three times greater than either the measured shift [Fig. 7(b)] or the calculated shift with the ponderomotive force included [Fig. 7(c)]. This translates into a difference in ZkT_e of a factor of approximately 10.

The ponderomotive pressure ($n_e m\langle v_{os}^2\rangle$) of the laser is enormous. Assuming the intensity and wavelength used in the experiment ($v_0/c \sim 0.05$) and critical density, it exceeds a Mbar. At higher intensity, it may reach the same order of magnitude as the thermal pressure associated with a fusion target. For this reason, this mechanism has also generated interest as a novel means of igniting thermonuclear fusion. Long-pulse lasers could heat and compress the fuel pellet through the usual ablation of the target. By the further heating and compression of the fuel with its enormous light pressure, an intense short-pulse laser may then be used as the ignitor.[34]

IV. SUMMARY

New ultra-high-intensity compact sources, three orders of magnitude brighter than previous ones, now make possible the study of laser–matter interactions in a fundamentally new regime. A variety of CPA-based lasers have now been developed with parameters suited to meet the requirements of many combinations of applications. Besides high intensity (10^{18} W/cm^2), these CPA-based lasers also provide short-pulse widths (100 fsec) for ultrafast studies and high average powers (up to 1 W) for the use of sampling techniques. They may also make compact coherent short-wavelength sources a real possibility within a few years. Already it has become possible to study, with these lasers, new issues in nonlinear optics involving free electrons. These include: multifoci formation, harmonic generation, and plasma dynamics dominated by light pressure. Undoubtedly, plenty of unexpected discoveries are yet in store now that this new research tool is widely available.

ACKNOWLEDGMENTS

We thank X. Liu, S. Coe, Y. Beaudoin, C. Chien, J. Tapie, F. Salin, and J. Squier for many important contributions; and E. Esarey and A. Ting for useful discussions.

This work was partially funded by National Science Foundation Center for Ultrafast Optical Science Contract No. PHY8920108, and the Office of Naval Research under Contract No. N00014-91-K-2005.

[1] P. Maine, D. Strickland, P. Bado, M. Pessot, and G. Mourou, IEEE J. Quantum Electron. **QE-24**, 398 (1988).
[2] W. Koechner, *Solid-State Laser Engineering* (Spring-Verlag, Berlin, 1988), p. 547.
[3] A. E. Siegman, *Lasers* (University Science Books, Mill Valley, CA, 1986), p. 386.
[4] M. Born and E. Wolf, *Principles of Optics* (Pergamon, New York, 1970), p. 486.
[5] F. G. Patterson, R. Gonzales, and M. D. Perry, Opt. Lett. **16**, 1107 (1991).
[6] C. Sauteret, D. Husson, C. Rouyer, S. Seznec, S. Gary, G. Mourou, and A. Migus, in *Conference on Lasers and Electro-Optics, 1991* (Optical Society of America, Washington, DC, 1991), p. 228.
[7] K. Yamakawa, H. Shiraga, and Y. Kato, Opt. Lett. **16**, 1593 (1991).
[8] Y. Beaudoin, C. Y. Chien, J. S. Coe, J. L. Tapie, and G. Mourou, to appear in Opt. Lett. (1992).
[9] J. L. Tapie and G. Mourou, Opt. Lett. **17**, 136 (1992).
[10] R. Fedosejevs, R. Ottmann, R. Sigel, G. Kuhnle, S. Szatmari, and F. P. Schafer, Appl. Phys. B **50**, 79 (1990).
[11] Y. H. Chuang, D. D. Meyerhofer, S. Augst, H. Chen, J. Peatross, and S. Uchida, J. Opt. Soc. Am. B **8**, 1226 (1991).
[12] F. Salin, J. Squier, and M. Piché, Opt. Lett. **16**, 1670 (1991); D. Negus, L. Spinelli, N. Goldblatt, and G. Feuguet, in *Digest of Meeting on Advanced Solid State Lasers* (Optical Society of America, Washington, DC, 1991), Paper No. PD-4; D. E. Spence, P. Kean, and W. Sibbett, Opt. Lett. **16**, 42 (1991).
[13] M. Hofer, M. E. Ferman, F. Haberl, M. H. Ober, and A. J. Schmidt, Opt. Lett. **16**, 502 (1991).
[14] O. E. Martinez, IEEE J. Quantum Electron. **QE-23**, 59 (1987).
[15] M. Pessot, P. Maine, and G. Mourou, Opt. Commun. **62**, 419 (1987).
[16] F. Salin, J. Squier, and G. Mourou, to appear in Appl. Opt.
[17] P. Bado (private communication).
[18] M. D. Perry, F. G. Patterson, and J. Weston, Opt. Lett. **7**, 381 (1990).
[19] F. Salin, C. Router, J. Squier, S. Coe, and G. Mourou, Opt. Commun. **84**, 67 (1991).
[20] G. Albrecht, A. Antonetti, and G. Mourou, Opt. Commun. **40**, 59 (1981).
[21] J. Squier, G. Mourou, F. Salin, and D. Harter, in Ref. 6, p. 228.
[22] J. Kmetec, J. J. Macklin, and J. F. Young, Opt. Lett. **16**, 1001 (1991).
[23] F. Salin, J. Squier, and G. Vaillancourt, Opt. Lett. **16**, 1964 (1992).
[24] D. Harter, E. Miller, R. Rapaport, J. Squier, and G. Mourou, in Proceedings of Optical Society of America Annual Meeting, 1991 (Optical Society of America, Washington, DC, to be published).
[25] D. Harter (private communication).
[26] J. Squier, G. Mourou, and D. Harter, in *Digest of Meeting on Advanced Solid State Lasers* (Optical Society of America, Washington, DC, 1991), p. 114.
[27] *Digest of Topical Meeting on High Energy Density Physics with Subpicosecond Laser Pulses, 1989* (Optical Society of America, Washington, DC, 1989).
[28] Special issue on "Atomic and Plasma Processes in X-Ray Lasers," IEEE Trans. Plasma Sci. **16**, 469–563 (1988).

[29]Special issue on "The Generation of Coherent XUV and Soft X-Ray Radiation," J. Opt. Soc. Am. B **4**, 530–609 (1987).
[30]X. F. Li, A. L'Huillier, M. Ferray, L. A. Lompre, and G. Mainfray, Phys. Rev. A **39**, 5751 (1989).
[31]J. F. Ward and G. H. C. New, Phys. Rev. **185**, 57 (1969); A. McPherson, G. Gibson, H. Jara, U. Johann, T. S. Luk, I. A. McIntyre, K. Boyer, and C. C. Rhodes, J. Opt. Soc. Am. B **4**, 595 (1987); K. C. Kulander and B. W. Shore, Phys. Rev. Lett. **62**, 524 (1989); M. Ferray, A. L'Huillier, X. F. Li, L. A. Lompré, G. Mainfray, and C. Manus, J. Phys. B **21**, L31 (1988); X. F. Li, A. L'Huillier, M. Ferray, L. A. Lompre, and G. Mainfray, Phys. Rev. A **39**, 5751 (1989); J. H. Eberly, Q. Su, and J. Javanainen, Phys. Rev. Lett. **62**, 881 (1989).
[32]X. Liu, D. Umstadter, J. S. Coe, C. Y. Chien, E. Esarey, and P. Sprangle, in *OSA Proceedings on Short Wavelength Coherent Radiation: Generation and Applications, 1991*, edited by P. Bucksbaum and N. Ceglio (Optical Society of America, Washington, DC, 1989), Vol. 11, pp. 32–34.
[33]D. Umstadter, X. Liu, J. S. Coe, and C. Y. Chien, in Ref. 32, pp. 55–57.
[34]M. Campbell (private communication).
[35]P. Sprangle, E. Esarey, and A. Ting, Phys. Rev. Lett. **64**, 2011 (1990); A. Ting, E. Esarey, and P. Sprangle, Phys. Fluids B **2**, 1390 (1990); P. Sprangle, E. Esarey, and A. Ting, Phys. Rev. A **41**, 4463 (1990).
[36]P. Sprangle, E. Esarey, A. Ting, and G. Joyce, Appl. Phys. Lett. **53**, 2146 (1988); E. Esarey, A. Ting, P. Sprangle, and G. Joyce, Comments Plasma Phys. Controlled Fusion **12**, 191 (1989).
[37]T. Tajima and J. M. Dawson, Phys. Rev. Lett **43**, 267 (1979); L. M. Gorbunov and V. I. Kirsanov, Zh. Eksp. Teor. Fiz. **93**, 509 (1987) [Sov. Phys. JETP **66**, 290 (1987)].
[38]V. L. Ginzburg, *Key Problems in Physics and Astrophysics* (MIR, Moscow, 1978), p. 78.
[39]J. D. Jackson, *Classical Electrodynamics* (Wiley, New York, 1975), p. 682.
[40]M. M. Murname, H. C. Kapteyn, and R. W. Falcone, in *Short Wavelength Coherent Radiation: Generation and Application*, edited by R. W. Falcone and J. Kirz (Optical Society of America, Washington, DC, 1989), Vol. 2, p. 189.
[41]J. C. Kieffer, P. Andebert, M. Chaker, J. P. Matte, A. Pépin, T. W. Johnston, P. Maine, D. Meyerhofer, J. Deletrez, O. Strickland, P. Bado, and G. Mourou, Phys. Rev. Lett. **62**, 760 (1989).
[42]W. L. Kruer, *The Physics of Laser Plasma Interactions* (Addison–Wesley, New York, 1988), p. 116.
[43]P. Amendt, D. C. Eder, and S. C. Wilks, Phys. Rev. Lett. **66**, 2589 (1991).
[44]N. Burnett and G. Enright, IEEE J. Quantum Electron. **QE-26**, 1797 (1990).
[45]S. Suckewer and C. H. Skinner, *Science*, March issue, 1553 (1990).
[46]F. Brunel, J. Opt. Soc. Am. B **7**, 521 (1990).
[47]E. S. Sarachik and G. T. Schappert, Phys. Rev. D **1**, 2738 (1970).
[48]S. Augst, D. D. Meyerhofer, C. I. Moore, and J. Peatross, in *Proceedings of SPIE OE/LASE '90*, Los Angeles, CA, January, 1990 (SPIE, Bellimgham, WA, 1990), Vol. 1229, p. 152.
[49]A. L'Huillier, L. A. Lompré, M. Ferray, X. F. Li, G. Mainfray, and C. Manus, Europhys. Lett. **5**, 601 (1988).
[50]D. S. Bethune, Phys. Rev. A **23**, 3139 (1981).
[51]M. Malcuit, R. W. Boyd, W. V. Davis, and K. Rzazewski, Phys Rev. A **41**, 3822 (1990).
[52]M. R. Cervenan, R. H. C. Chan, and N. R. Isenor, Can. J. Phys. **53**, 1573 (1975).
[53]J. Solem, T. S. Luk, and K. Boyer, IEEE J. Quantum Electron. **QE-25**, 2423 (1989).
[54]M. H. Sher, J. F. Macklin, J. F. Young, and S. E. Harris, Opt. Lett. **12**, 891 (1987).
[55]T. Afshar-rad, L. A. Gizzi, M. Desselberger, F. Khattak, O. Willi, and A. Giulietti, Phys. Rev. Lett. **68**, 942 (1992); P. E. Young, H. A. Baldis, T. W. Johnston, W. L. Kruer, and K. G. Estabrook, Phys. Rev. Lett. **63**, 2812 (1988); P. E. Young, R. P. Drake, E. M. Campbell, and K. G. Estabrook, Phys. Rev. Lett. **61**, 2336 (1988); M. J. Herbst, J. A. Stamper, R. R. Whitlock, R. H. Lehmberg, and B. H. Ripin, Phys. Rev. Lett. **46**, 328 (1981); R. Craxton and R. L. McCrory, J. Appl. Phys. **56**, 108 (1984).
[56]Y. R. Shen, *The Principles of Nonlinear Optics* (Wiley, New York, 1984).
[57]C. Max, J. Arons, and A. B. Langdon, Phys. Rev. Lett. **33**, 209 (1974); G. Z. Sun, E. Ott, Y. C. Lee, and P. Guzdar, Phys. Fluids **30**, 526 (1987); P. Sprangle, C. M. Tang, and E. Esarey, IEEE Trans. Plasma Sci. **PS-15**, 145 (1987); A. Borisov, A. V. Borovskiy, O. B. Shiryaev, V. V. Korobkin, A. M. Prokhorov, J. C. Solem, T. S. Luk, K. Boyer, and C. K. Rhodes, to appear in Phys. Rev. A.
[58]I. Golub, Y. Beaudoin, and S. L. Chin, J. Opt. Soc. Am. **B5**, 2490 (1988).
[59]D. Umstadter, H. Milchberg, T. McIlrath, and R. R. Freeman, in *Digest of Topical Meeting on High Energy Density Physics with Subpicosecond Laser Pulses, 1989* (Optical Society of America, Washington, DC, 1989), pp. 89–93.
[60]J. C. Kieffer, J. P. Matte, S. Belair, M. Chaker, P. Andebert, A. Pépin, P. Maine, D. Strickland, P. Bado, and G. Mourou, IEEE J. Quantum Electron. **QE-25**, 2640 (1989).